

Rotation-Infall Motion around the Protostar IRAS 16293-2422 Traced by Water Maser Emission

Hiroshi IMAI

Mizusawa Astrogeodynamics Observatory, National Astronomical Observatory, Mizusawa, Iwate 023-0861

E-mail (HI): imai@miz.nao.ac.jp

Takahiro IWATA*

Kashima Space Research Center, Communications Research Laboratory, Kashima, Ibaraki 314-0012

and

Makoto MIYOSHI

VERA Project Office, National Astronomical Observatory, Mitaka, Tokyo 181-8588

(Received 1999 April 26; accepted 1999 May 17)

Abstract

We made VLBI observations of the water maser emission associated with a protostar, IRAS 16293—2422, using the Kashima-Nobeyama Interferometer (KNIFE)t and the Japanese domestic VLBI network (J-Net). * These distributions of water maser features showed the blue-shifted and red-shifted components separated in the north-south direction among three epochs spanning three years. The direction of the separation was perpendicular to the molecular outflow and parallel to the elongation of the molecular disk. These steady distributions were successfully modeled by a rotating-infalling disk with an outer radius of 100 AU around a central object with a mass of 0.3 M \odot . The local specific angular momentum of the disk was calculated to be 0.2-1.0 $\times 10^{-3}$ km s $^{-1}$ pc at a radius of 20-100 AU. This value is roughly equal to that of the disk of IRAS 00338+6312 in L1287 and those of the molecular disks around the protostars in the Taurus molecular cloud. The relatively large disk radius of about 100 AU traced by water maser emission suggests that impinging clumps onto the disk should be hotter than 200 K to excite the water maser emission.

Key words: Masers — Stars: formation — Stars: mass accretion — Stars: individual [IRAS 16293-2422 (*p* Oph East)]

1. Introduction

Water maser emission in star-forming regions is a good tracer of gas kinematics in the very vicinity of protostars. Most of these water masers are associated with molecular outflows (see reviews of Elitzur 1992; Bachiller 1996). Recent observations have found water masers associated with compact (< 100 AU) gas disks around protostars (IRAS 00338+6312 in L1287, Fiebig et al. 1996; Cep A HW 2, Torrelles et al. 1996; NGC 2071 IRS 3, Torrelles et al. 1998). Since circumstellar disks are considered to play important roles in transferring material from circumstellar envelopes to the central protostars (e.g., Shu

et al. 1987), the rotation and infall motions of the disks provide clues to elucidate the gas dynamics at very early stages of star formation.

The low-mass protostar IRAS 16293-2422 (*d* = 160 pc, Whittet 1974), associated with a molecular outflow *p* Oph East (Mizuno et al. 1990), is a candidate of a protostar showing contraction motion on a scale of 0.03 pc (e.g., Narayanan et al. 1998). Water maser emission is also associated with the radio continuum source IRAS 16293-2422 A (Wootten 1993; Mundy et al. 1992; Estalella et al. 1991).

In this paper, we present the results obtained from the Kashima-Nobeyama Interferometer (KNIFE) and the Japanese domestic VLBI network (J-Net). We found a similar velocity distribution of maser features among three epochs spanning three years. It is likely that these steady distributions reflect the constant characteristics of the kinematics in this region.

We attempted an interpretation of the maser feature distributions using the rotating-contracting disk model proposed by Cassen and Moosman (1981), which has suc-

* Present address: Office of Research & Development, National Space Development Agency of Japan, Tsukuba, Ibaraki 305-8505.

t Mizusawa, Nobeyama, and Kagoshima stations are operated by staff members of National Astronomical Observatory of the Ministry of Education, Science, Sports and Culture. Kashima station is operated by staff members of Communications Research Laboratory of the Ministry of Posts and Telecommunications. The recent status of J-Net is seen in the WWW home page: <http://www.nro.nao.ac.jp/~miyajii/Jnet>.

cessfully explained the velocity distribution of the LI287 water maser (Fiebig 1997).

2. Observations and Data Reduction

We performed three epochs of VLBI observations on 1991 May 28 using KNIFE (e.g., Miyoshi et al. 1993) and on 1994 April 5 and June 1 using J-Net (e.g., Omodaka et al. 1994). KNIFE and J-Net have minimum fringe spacings of 14 milliarcseconds (mas) and 2.1 mas at the 22.2 GHz band, respectively. The received signals were recorded using a K-4 backend system (Kiuchi et al. 1991), which has 16 video channels, each with a 2 MHz bandwidth.

The recorded data were correlated using the New Advanced One-unit Correlator (NAOCO) (Shibata et al. 1994), whose outputs have 256 channels in the cross-power spectrum with 0.1 km s^{-1} velocity spacing each at the 22.2 GHz band.

We performed a multiple-point fringe-rate mapping analysis (Walker 1981) in order to obtain wide-field ($\sim 2''$) maps. We selected velocity channels with the strong single maser spots ($\text{VLSR} = 7.9 \text{ km s}^{-1}$, $S_u \sim 210 \text{ Jy}$ on 1991 May 28 and $\text{VLSR} = 1.9 \text{ km s}^{-1}$, $S_u \sim 230$ to 650 Jy on 1994 April 5 and June 1) as fringe-phase references. The correlated data of all velocity channels were integrated in the phase-referencing mode for 1000 to 1200 seconds to obtain an appropriate number of fringe-rate $\langle \dot{\phi}(u,v) \rangle$ data sets with a sensitivity of approximately 2 Jy at the $7\text{-}\sigma$ level and a spatial resolution of 140 mas and 60 mas in KNIFE and J-Net, respectively. We thus obtained fringe-rate maps with a typical relative position accuracy of 5 to 15 mas in right ascension and 7 to 20 mas in declination in all of the maps. Figure 1 shows the fringe-rate maps of the water maser emission of IRAS 16293–2422 at three epochs spanning three years.

3. Results

Water maser emission appeared in the velocity coverage of $-8 \text{ km s}^{-1} < \text{VLSR} < 8 \text{ km s}^{-1}$ during the three epochs. Figure 1 indicates that (a) the blue-shifted ($-8 \text{ km s}^{-1} < \text{VLSR} < 1 \text{ km s}^{-1}$) and red-shifted ($4 \text{ km s}^{-1} < \text{VLSR} < 8 \text{ km s}^{-1}$) components were always separated in the north-south direction by $\sim 0.5''$, and (b) in the red-shifted components, the velocity gradient in the northeast-southwest direction always appeared with a length of about $0.3''$.

In the low-mass star-forming regions, the lifetime of each water maser feature was estimated to be typically 1–2 months (Claussen et al. 1996). Therefore, it is expected that the spatial distributions of the water maser features change temporarily in the steady kinematics, which is called the "Christmas-tree effect" (Gwinn et al. 1992). Therefore, we superposed these maps in order to find

steady kinematics based on the assumption that compact groups of strong maser features ($> 40 \text{ Jy}$) with a velocity of around $\text{VLSR} = 7 \text{ km s}^{-1}$ in each map always exist at almost the same position in the sky. The superposed map is shown in figure 2.

Other characteristics of the velocity distribution are also revealed in figure 2 as follows: (c) The extremely blue-shifted components ($\text{VLSR} < -5 \text{ km s}^{-1}$) exist in the inner part of the blue-shifted components, (d) The red-shifted components have a relatively simple and small velocity gradient in the northeast-southwest direction. (e) The intermediate velocity components ($1 \text{ km s}^{-1} < \text{VLSR} < 4 \text{ km s}^{-1}$) and blue-shifted components appear temporarily at the west and east sides of the overall distribution of the water maser emission.

4. Discussion

The direction of the separation between the blue-shifted and red-shifted components is roughly perpendicular to the direction of the CO outflow with a scale of 0.5 pc (Wed-Ebiue direction in Mizuno et al. 1990) and parallel to the elongation axis of the C^{18}O emission (Mundy et al. 1990). This suggests that our observed water masers can be associated with a circumstellar disk rotating around the central protostar. We attempted to explain the velocity distribution of the water maser features using three kinematical models for the disk: infall plus rotation, pure Keplerian rotation, and Keplerian rotation plus radial expansion.

For the first model, we used the same velocity-field model of the rotating-infalling disk proposed by Cassen and Moosman (1981) and Fiebig (1997). This model proposes a thin disk and gas clumps which move in the trajectory planes with a specific angle with respect to the disk-rotation axis and impinge onto the disk. The mass of the disk is assumed to be negligible in this model. Water maser emission is expected to be excited on the disk where an infalling gas clump collides with the disk and reaches an appropriate physical condition for maser excitation ($T \sim 400 \text{ K}$ and $mn_2 \sim 10^9 \text{ cm}^{-3}$) created by shock. The velocity field of the disk (v_r , V_Q , V^\wedge) is calculated using the zero-energy orbits of the impinging clumps on parabolas, and is expressed in the spherical coordinate system as follows:

$$v_r = -(GM_+/r_n)^{1/2}, \quad (1)$$

$$\wedge = (GM^*/r_i)^{1/2} \cos \wedge_0, \quad (2)$$

$$\wedge = (GM^*/r_i)^{1/2} \sin \wedge_0, \quad (3)$$

where M^* is the mass of the central stellar object, n is the distance from the stellar object on the disk, and \wedge_0 is the angle between the disk-rotation axis and the trajectory plane of the impinging clump. Here, \wedge_0 monotonically

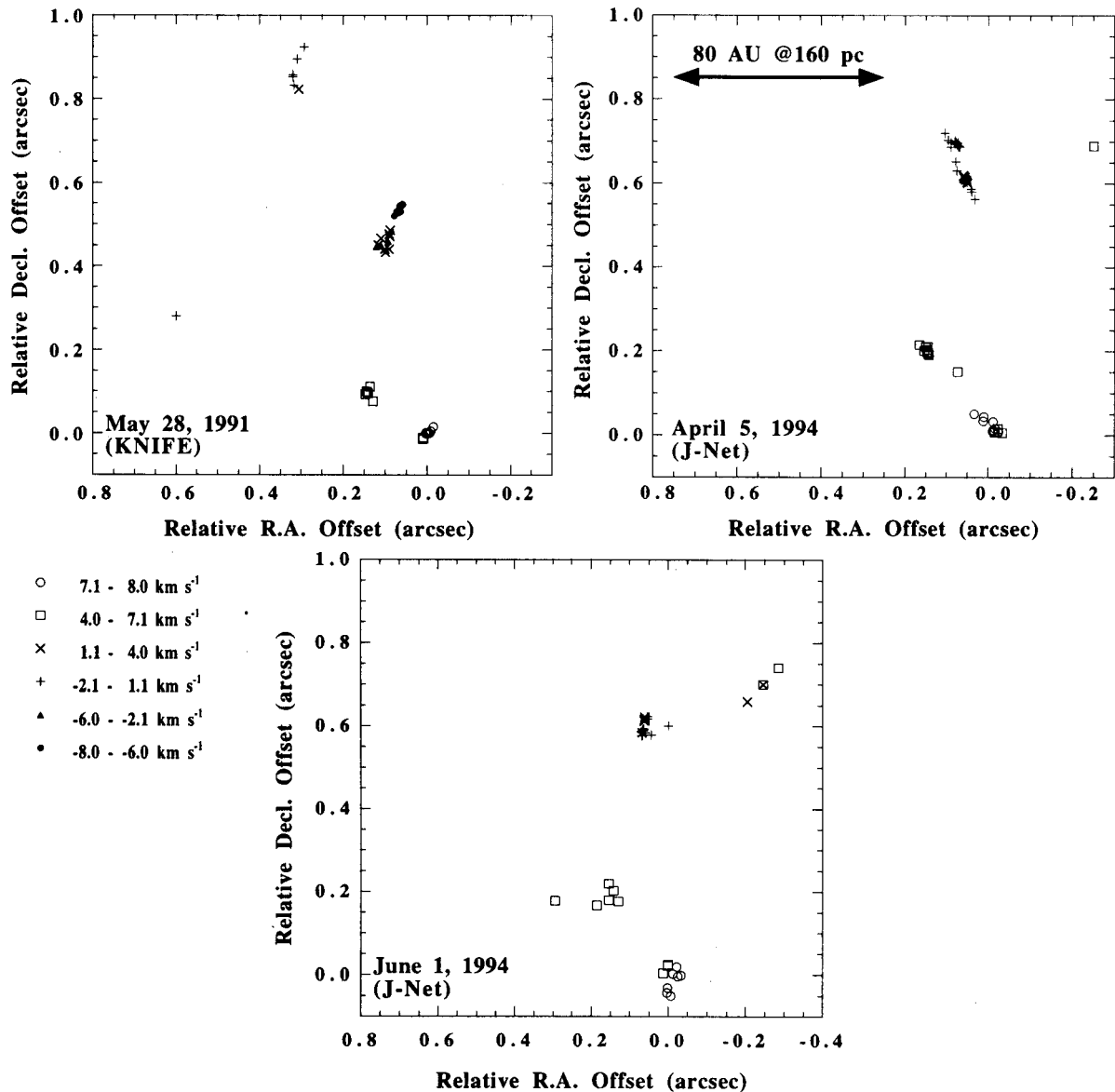


Fig. 1. Distributions of the water maser emission at three epochs: Left, on 1991 May 28; Right, on 1994 April 5; Middle, on 1994 June 1. The origin of each map is at the mean position of the maser spots with line-of-sight velocities around $V_{\text{LSR}} = 7.0 \text{ km s}^{-1}$ which was roughly estimated as R.A. (B1950) = $16^{\text{h}}29^{\text{m}}2^{\text{s}}.02$, Decl. (B1950) = $-24^{\circ}22'16''.2$.

increases with r_x as,

$$\sin^2 \theta_0 = n/rd, \quad (4)$$

where r is the distance from the protostar, which gives $\theta_0 = 0$. After colliding with the disk, the velocity vector of the impinging clump loses the \hat{z} -component in equation (2) on the disk.

We assumed a systemic velocity of the IRAS 16293-2422 system as $V_{\text{LSR}} = 4 \text{ km s}^{-1}$, which is cited from the observational results of Narayanan et al. (1998)

and Zhou (1995). The best-fit model for the IRAS 16293-2422 water maser shown in figure 3 (Plate 22) well explains all of the characteristics of the velocity distribution of (a)-(e) in section 3. We obtained the following best parameter set: the stellar position at (0."06, 0."49) in figure 2, $M^* = 0.3 M_{\odot}$, $r^{\wedge} = 300 \text{ AU}$, the inclination and position angles of the disk-rotation axis of $\delta = -55^{\circ}$ and P.A. = 80° , respectively.

The derived P.A. value is almost equal to the inner 5000 AU of CO outflow driven by IRAS 16293-2422 A

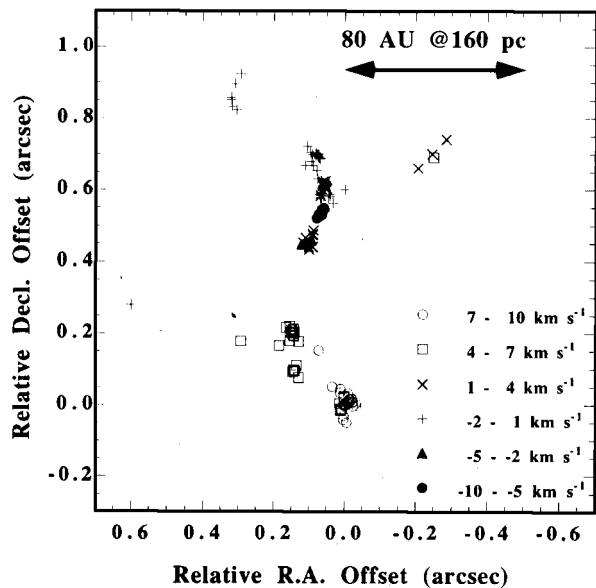


Fig. 2. Distribution of the water maser emission obtained by superposing the maps of the three epochs shown in figure 1.

recently observed using the Nobeyama Millimeter Array (Hirano et al. 1999 in private communication). Most of the maser features exist within 100 AU from the assumed position of the protostar. It is uncertain whether the maser feature at the eastern edge of figure 2 is associated with the disk.

The estimated mass of the central protostar is about $0.3 M_{\odot}$, which is consistent with that estimated from the mass-accretion rate ($\dot{M}^* \sim 0.27 M_{\odot}$ for $\dot{M} \sim 2.9 \times 10^{-5} M_{\odot} \text{ yr}^{-1}$, Narayanan et al. 1998). The dynamical mass of the infalling molecular core ($r \sim 6000$ AU) is estimated as about $2.3 M_{\odot}$ (Narayanan et al. 1998). These suggest that IRAS 16293-2422 is in early phase of star formation, where most of the mass is included in the circumstellar envelope. Considering the volume of the maser-associating disk ($r \sim 100$ AU), the disk mass is negligible compared to the protostar mass in such a small volume.

We also applied the two other kinematical models mentioned above. These models and the kinematical characteristic (c) largely mismatch. The position angles of the disk-rotation axis of the obtained models ($\sim 110^{\circ}$ and 160° , respectively) and direction of the CO outflow ($\sim 90^{\circ}$) are also inconsistent. Thus, the contraction motion of the disk should be taken into account.

Ohashi et al. (1997) found that circumstellar molecular gases rotating and contracting around the central protostars roughly show a constant local specific angular momentum ($\sim 10^{-3} \text{ km s}^{-1} \text{ pc}$) within 0.03 pc in low-

mass young stellar objects. In our results, the velocity distribution of the water maser features associated with IRAS 16293-2422 suggests a local specific angular momentum of $0.2\text{--}1.0 \times 10^{-3} \text{ km s}^{-1} \text{ pc}$ at a distance of 20-100 AU from the protostar. We estimated this value to be $1.6 \times 10^{-3} \text{ km s}^{-1} \text{ pc}$ for the disk of the L1287 water maser at the outer edge of the disk ($r = 35$ AU in Fiebig 1997). These values are consistent with the results of a statistical analysis for circumstellar disks (Ohashi et al. 1997), and suggest that the local specific angular momenta in circumstellar disks are kept at $\sim 10^{-3} \text{ km s}^{-1} \text{ pc}$ in a scale range larger than two orders of magnitude (from 30 AU to 6000 AU).

In addition, the basic kinematics of the disk-impinging-clump model which we applied is consistent with the interpretation of the observational result as "dynamical collapse" by Ohashi et al. (1997) and a model proposed by Momose et al. (1998), which is applied to molecular disks traced by several molecular emission lines. Momose et al. (1998) considered a similar kinematic model which takes into account the density profile of a circumstellar envelope and the brightness distribution of the line emission, and succeeded to explain the observational result of a molecular disk around L1551 IRS 5.

For water maser emission in the accretion disk, we must also take into account the maser excitation condition, which has been expressed by Fiebig (1997). In the assumed temperature of impinging clumps of 100 K (Butner et al. 1994), the Λ -component should be larger than 4.2 km s^{-1} to create a shocked gas hotter than 400 K for water maser excitation (Fiebig 1997). The distance from the protostar corresponding to the above Λ -component derived from equation (2) is smaller than 80 AU. A clump temperature higher than 200 K should be considered to explain the larger maser feature distribution in this region (~ 100 AU). This is consistent with a result of Ceccarelli et al. (1998), which suggests the existence of a diffuse hot gas with a temperature much larger than 150 K.

Some weaker maser features, detected in only one epoch, mismatch with our applied model in the line-of-sight velocities by 1 to 3 km s^{-1} . There were similar maser features of weaker than 1 Jy in 1989 January obtained by Wootten (1993), which seem to have been random in space. It is likely that these maser features were excited by outflow from the protostar, as suggested by Wootten (1993), while the distributions of the stronger maser features which we detected were roughly consistent with that of the stronger maser features obtained by Wootten (1993). Our results show steady kinematics in this region reflected on the stronger water maser features.

It is also important to investigate the gas kinematics close to the protostar on a scale smaller than 10 AU. Some water maser features in IRAS 16293-2422 are

expected to exist in such a compact region [figure 3 (Plate 22)]. As future work, we plan to perform phase-synthesis imaging with a positional accuracy better than one milliarcsecond. It is expected from our proposed model that relative proper motions of 1 mas per month, or transverse velocities of 10 km s^{-1} , were measured among the water maser features between 1994 April 5 and June 1.

We acknowledge the staff members and students of KNIFE and J-Net for their help in operating of the telescopes. The staff members of KRC/CRL deeply contributed to the KNIFE/J-Net observations. The staff members of Mizusawa Astrogeodynamics Observatory/NAO helped us in the data correlation. We also thank Drs. T. Umemoto, N. Hirano, and T. Sasao for giving fruitful comments. H. I. was financially supported by the Research Fellowship of the Japan Society for the Promotion of Science for Young Scientist.

References

- Bachiller R. 1996, *ARA&A*, 34, 111
 Butner H.M., Natta A., Evans N.J. II 1994, *ApJ* 420, 326
 Cassen P., Moosman A. 1981, *Icarus* 48, 353
 Ceccarelli C, Caux E., White G.J., Molinari S., Furniss I., Liseau R., Nisini B., Saraceno P. et al. 1998, in *Star Formation with the Infrared Space Observatory*, ed J.L. Yun, R. Liseau, ASP Conf. Ser. 132, p243
 Claussen M.J., Wilking B.A., Benson P.J., Wootten A., Myers P.C., Terebey S. 1996, *ApJS* 106, 111
 Elitzur M. 1992, *ARA&A* 30, 75
 Estalella R., Anglada G., Rodriguez L.F., Garay G. 1991, *ApJ* 371, 626
 Fiebig D. 1997, *A&A* 327, 758
 Fiebig D., Duschl W.J., Menten K.M., Tschanuter W.M. 1996, *A&A* 310, 199
 Gwinn C.R., Moran J.M., Reid M.J. 1992, *ApJ* 393, 149
 Kiuchi H., Hama S., Amagai J., Abe Y., Sugimoto Y., Takahashi F., Kawaguchi N. 1991, in *Proc. the AGU Chapman Conference on Geodetic VLBI: Monitoring Global Change*, NOAA Technical Report NOS 137, p35
 Miyoshi M., KNIFE team 1993, in *Astrophysical Masers*, ed A.W. Clegg, G.E. Nedoluha (Springer-Verlag, Heidelberg) p441
 Mizuno A., Fukui Y., Iwata T., Nozawa S., Takano T. 1990, *ApJ* 356, 184
 Momose M., Ohashi N., Kawabe R., Nakano T., Hayashi M. 1998, *ApJ* 504, 314
 Mundy L.G., Wootten H.A., Wilking B.A. 1990, *ApJ* 352, 159
 Mundy L.G., Wootten H.A., Wilking B.A., Blake G.A., Sargent A.I. 1992, *ApJ* 385, 306
 Narayanan G., Walker C.K., Buckley H.D. 1998, *ApJ* 496, 292
 Ohashi N., Hayashi M., Ho P.T.P., Momose M., Tamura M., Hirano N., Sargent A.I. 1997, *ApJ* 488, 317
 Omodaka T., Morimoto M., Kawaguchi N., Miyaji T., Yasuda S., Suzuyama T., Kitagawa T., Miyazaki T. et al. 1994, in *VLBI Technology, Progress and Future Observational Possibilities*, ed T. Sasao, S. Manabe, O. Kameya, M. Inoue (Terra Scientific Publishing Company, Tokyo) p191
 Shibata K.M., Sasao T., Kawaguchi N., Tamura Y., Kamenno S., Miyoshi M., Asari K., Manabe S. et al. 1994, in *VLBI Technology, Progress and Future Observational Possibilities*, ed T. Sasao, S. Manabe, O. Kameya, M. Inoue (Terra Scientific Publishing Company, Tokyo) p327
 Shu F.H., Adams F.C., Lizano S. 1987, *ARA&A* 25, 23
 Torrelles J.M., Gomez J.F., Garay G., Rodriguez L.F., Curiel S., Cohen R.J., Ho P.T.P. 1998, *ApJ* 509, 262
 Torrelles J.M., Gomez J.F., Rodriguez L.F., Curiel S., Ho P.T.P., Garay G. 1996, *ApJ* 457, L107
 Walker R.C. 1981, *AJ* 86, 1323
 Whittet D.C.B. 1974, *MNRAS* 168, 371
 Wootten A. 1993, in *Astrophysical Masers*, ed A.W. Clegg, G.E. Nedoluha (Springer-Verlag, Heidelberg) p441
 Zhou S. 1995, *ApJ* 442, 685

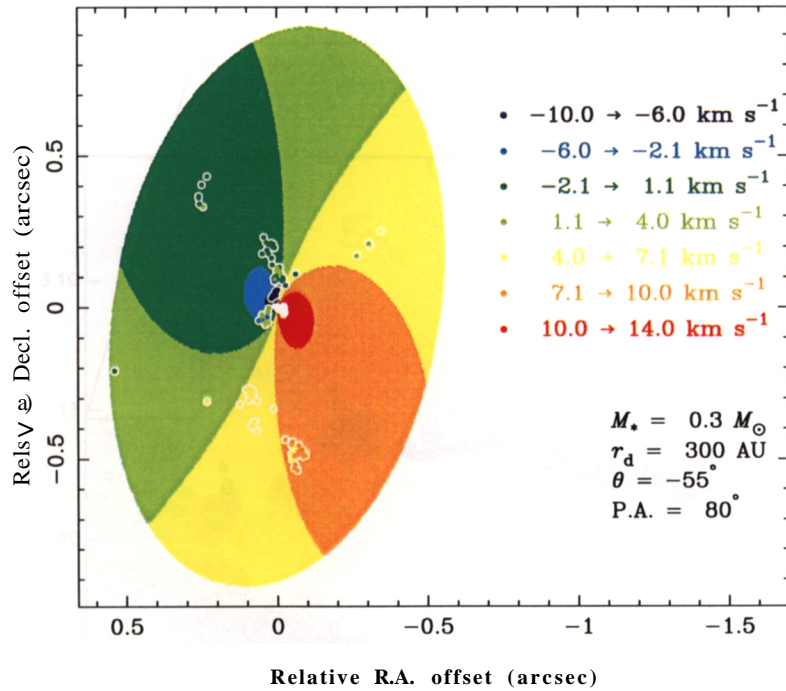


Fig. 3. Calculated LSR-velocity distribution for masing gas of clumps impinging onto an initially thin disk. Here, M^* is the mass of the central stellar object, r^{\wedge} is the distance from the protostar, which gives the angle between the disk rotation-axis and the trajectory plane of the clump $9Q = 0$, as shown in equation (4), δ is the inclination of the disk with respect to the line-of-sight, and P.A. is the position angle of the disk. The map origin is at the assumed position of the protostar. The outer disk edge is truncated at 150 AU. The systemic velocity is assumed as $V_{\text{LSR}} = 4 \text{ km s}^{-1}$. The water maser spots displayed in figure 2 (dots) are overlaid after shifting the offset coordinates by $(-0''06, -0''49)$.

H. IMAI, T. IWATA, and M. MIYOSHI (See Vol. 51, 475, 477)